Opto-Electronic Engineering

Article
2017, Vol 44, Issue 1

Ultra-broadband terahertz polarization transformers using dispersion-engineered anisotropic metamaterials

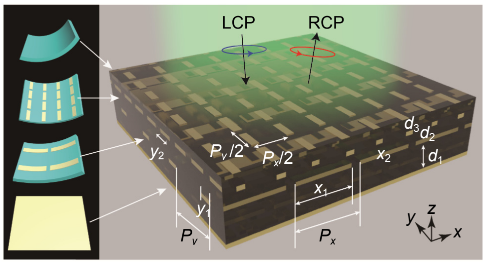

Po Chen

Department of Geology and Geophysics, University of Wyoming, Laramie, Wyoming 82071, USA

Abstract: We propose the design of anisotropic metamaterials with cascading meta-atoms. Each meta-atom array behaves as an impedance-tuned interface and dramatically modifies the complex reflection and transmission coefficients. By engineering the frequency-dependent impedances, the reflection phase difference along the two axes of anisotropic metamaterials approximates to a constant in a wide range. We numerically demonstrate the proposed anisotropic metamaterials can accomplish achromatic polarization transformation from 0.5 THz to 3.1 THz. The polarization conversion ratio is higher than 80%, which exhibits excellent agreements with the theoretical calculation. Such design is scalable to other bands and can provide helpful guidance in broadband devices design.

Keywords: polarization conversion; terahertz; cascaded meta-atoms array

DOI: 10.3969/j.issn.1003-501X.2017.01.008 **Citation:** *Opto-Elec Eng*, 2017, **44**(1): 82−86

1 Introduction

The ability to manipulate the polarization of electromagnetic waves is sought-after for numerous applications. Traditional polarization rotation devices utilizing natural occurring birefringence or total internal reflection effects are bulky. As an alternative solution, metamaterial-based converters exhibiting strong anisotropy or chiral can be extremely compact and thus flourished in the last decade [1-3]. Nevertheless, metamaterial-based schemes suffer from the complex fabrication technology and tremendous loss. The gradient phase metasurface, because of the reduced dimension and loss as well as powerful phase engineering ability, is taken as a promising approach for polarization manipulation [4-9]. Traditional metasurfaces are composed of discrete meta-atoms and the phase profile is approximated by several levels of phase discontinuities, which inevitably degrades the overall performance of metasurfaces. Quite recently, semicontinuous super-meta-atoms including catenary[10-11] and trapezoid shaped structure[12] as well as truecontinuous super-meta-atoms including annular slits[13-14] and sinusoidal metallic strips[15] are adopted in metasurfaces to overcome the shortages above.

However, most existing metasurfaces also suffer from narrow bandwidth due to their highly dispersive meta-molecules. Many excellent attempts were carried out to extend the working bandwidth in different frequency regimes[16]. The most direct way is superimposing different resonance modes within a unit cell[17-18]. For example, Cui et al. have proposed a broadband half-wave retarder consisting of multi-layer non-resonant meta-molecule in gigahertz frequency[19]. By stacking periodically multi-layered structures comprising of two different types of arrays of nanorods, Jen et al. have experimentally demonstrated a broadband wave plate at visible frequencies[20]. However, the extended operation bandwidth is at a cost of increased physical thickness, ruled by the thickness-to-bandwidth ratio limit presented by Romanov[21].

To overcome this issue, the metasurface-assisted Fresnel's equation is proposed[5-6]. Following the general strategy of dispersion engineering[22-24], ultra-broadband polarization conversion were obtained[25-27], demonstrating unprecedented performance compared with traditional devices. The bandwidth-thickness limit of the perfect absorber and waveplate is also unified with the above principle [25]. It was shown that the thickness of broadband waveplates could be suppressed close to or even below the classic limit set by Max Planck almost a century ago[5].

Achromatic polarization converters operating in the

Received 12 October 2016; accepted 10 December, 2016
E-mail: pchen@uwyo.edu

DOI: 10.3969/j.issn.1003-501X.2017.01.008

terahertz band are highly anticipated due to the lack of suitable natural materials for terahertz device applications[28-29]. If the dispersion is engineered properly so that the thickness-dependent dispersion of the dielectric spacing layer can be conjugated cancelled by the dispersion of metasurface, the operation bandwidth can be extended to octave scale [25-26, 30-32]. In this paper, we proposed an ultra-broadband terahertz transformer with cascaded meta-atoms, in which dispersions are dedicatedly engineered. Both theoretical and numerical results demonstrated the bandwidth of our proposed transformer exceeds 2-octave.

2 Theory

Fig.1 illustrates a schematic concept of broadband polarization-transforming electromagnetic mirror constructed by alternately stacked metallic cut-wires with orthogonal orientation and each polarized set is arranged in a log-periodic configuration [33-34]. The scaling factor that governs the relation between consecutive antenna dimension and location is defined as τ. According to the transmission line circuit theory, the phase of the reflection coefficient of each set of arrays varies essentially linearly with the logarithm of frequency as follows [35]:

$$\phi_x = \phi_0 - (2\pi / \log\tau)\log(f / f_x) \quad , \tag{1}$$

$$\phi_y = \phi_0 - (2\pi / \log\tau)\log(f / f_y) \quad , \tag{2}$$

where ϕ_0 is constant, f is the incidence frequency, f_x and f_y are the resonant frequencies of X- and Y- polarized array. The phase difference between them is expressed as:

$$\Delta\phi = (2\pi / \log\tau)\log(f_x / f_y) \quad . \tag{3}$$

From equation (3), we find the phase difference is frequency-independent, which is only a function of the scale factor ρ between adjacent orthogonally polarized arrays. By adjusting the scale factor, arbitrarily polarization state can be achieved. Specially, if $\rho = \tau^{1/2}$ ($\tau^{1/4}$), $\Delta\phi = \pi$ ($\pi/2$) achromatic half- (quarter-) wave plate is realized.

Enlightened by the conceptual configuration above, we design an achromatic transformer, which is composed of a dielectric coating layer, two meta-atoms array deposited on dielectric substrate, and a metallic reflection plane, as sketched in Fig. 2. For clarity of contents, the upper and lower meta-atoms arrays are denoted by subscripts 1 and 2, respectively. Each metasurface is composed of subwavelength metallic cut-wire array and the lateral period of the metasurface 2 is twice of the metasurface 1. The metallic parts are made of gold with thickness of 0.25 μm. Polymide dielectric spacer has a relative dielectric permittivity $\varepsilon_r \sim 3$ and a moderate loss tangent $\tan\delta \sim 0.005$[31]. In the design process, we first consider a meta-mirror with the single metasurface, in which geometric parameters are optimized by parameters sweep. Then another metasurface can be easily obtained by scaling the first one and rotating it with an angle of 90°[27]. The final optimal geometrical parameters of proposed meta-mirror for achromatic polarization manipulation can be quickly obtained with further numerical simulations.

3 Simulation

In order to check the performance of the proposed meta-mirror, numerical simulation is performed within CST Microwave Studio. In the simulation, unit cell boundary condition is adopted along x and y directions, whereas the open boundary condition is applied for z direction. To function as a half-wave plate, the geometric parameters of meta-mirror are optimized as P_x = 68 μm, P_y = 57 μm, x_1 = 67 μm, y_1 = 13 μm, x_2 = 8 μm, y_2 = 23 μm, d_0 = 24 μm, d_1 = 13 μm, d_2 =31 μm. A left-handed circularly

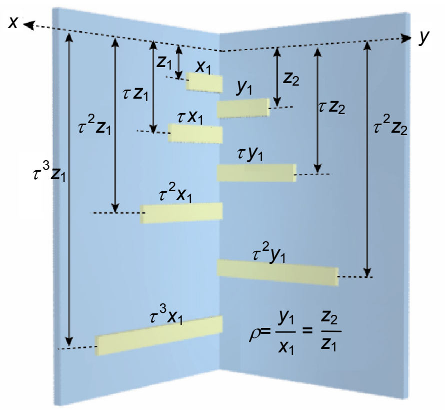

Fig.1 Schematic concept of wideband polarization-transforming electromagnetic mirror based on log-periodic antennas.

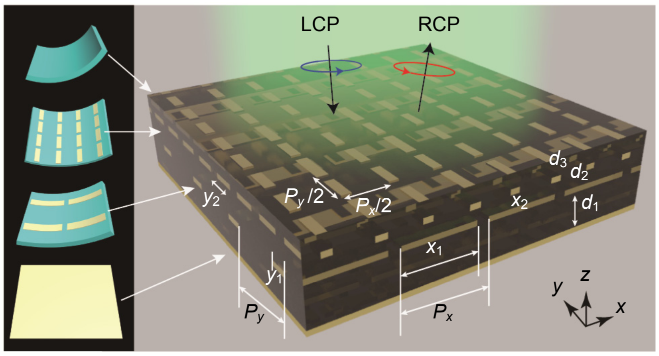

Fig.2 Schematic of the proposed anisotropic meta-mirrors for achromatic polarization manipulation, which is constructed by two meta-atoms array and a metallic reflection plane separated by dielectric spacers. The dielectric thicknesses from top to bottom are d_0, d_1 and d_2, respectively. The period of the metasurface is (P_x/2, P_y/2) and (P_x, P_y) for the upper one and bottom one, respectively.

polarized (LCP) plane wave is normally incident on the sample, which is likely to achromatically convert its polarization to right-handed circularly polarized (RCP) after the reflection, where the handedness of the circular polarization is defined from the source plane.

The simulated circular polarization reflectance is presented in Fig. 3(a). It can be found that the opposite-polarized reflection carries more than 80% of the incident power in the range of 0.5~3.1 THz (beyond 2-octave bandwidth), while the co-polarized component is mostly below 20%. The polarization conversion ratio (PCR) is also calculated and plotted in Fig. 3(b). We can see the PCR is larger than 0.8 in the range of 0.5~1.8 THz, and larger than 0.9 in the range of 1.8~3.1 THz. Especially, the LCP is totally converter to the RCP at six frequency points of 0.54 THz, 1.1 THz, 1.9 THz, 2.2 THz, 2.5 THz, and 3 THz. Obviously, our design has superiorities compared with the previous couterparts. Initially, the bandwidth is beyond 2-octave, about three times of previous design. Moreover, there is no extra process to ensure the alignment between the two meta-atoms array, which releases the fabrication requirements.

4 Analysis

Fig.4 reveals the anisotropic reflection phase of the meta-mirror, from which we can see the phase difference (red solid line) fluctuates around desired −180° (-160°, -210°) in the operation band. Outside of the operation band, the phase retardation severely changes to 0 or -360°. There are six intersections between the phase difference and the -180°, which correspond to the six conversion peaks above.

Subsequently, we resort to the transmission line model (TLM) to illustrate the underlying physical mechanism of polarization manipulation, where we consider the presence of the metal array as a thin impedance sheet, as illustrated in Fig. 5. Ignoring the loss, the metallic cut-wire can be taken regarding as a combination of an effective inductor and capacitor, in which impedance is expressed as:

$$Z_{1(2),x(y)} = \mathrm{j}\omega L_{1(2),x(y)} + 1/\,\mathrm{j}\omega C_{1(2),x(y)} \qquad (4)$$

To fit the anisotropic dispersions in Fig. 4, the effective circuit parameters are estimated as $(L_{1,x}, C_{1,x}) = (2\times10^{-12}$ H, 5×10^{-17} F), $(L_{1,y}, C_{1,y}) = (7.5\times10^{-12}$ H, 2.8×10^{-16} F),

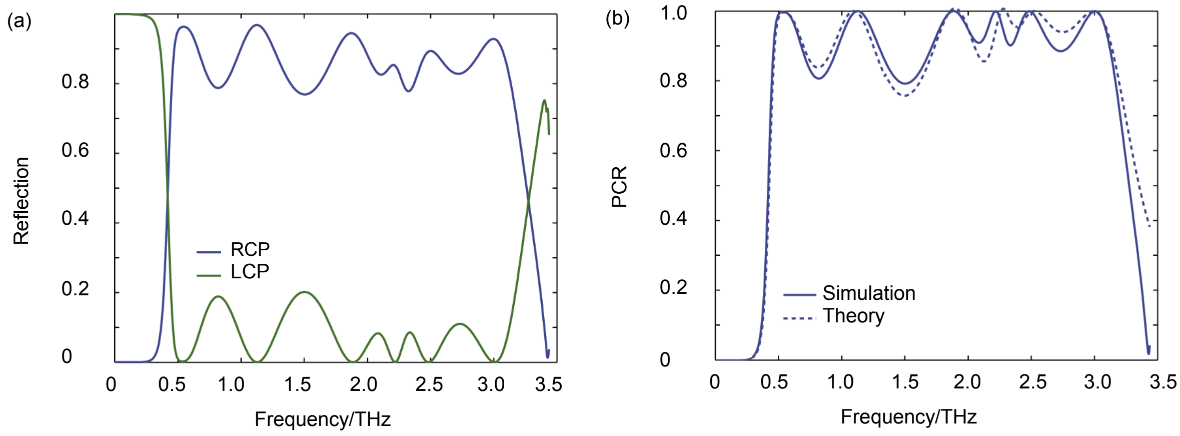

Fig.3 (a) Simulated reflectance of the co- and opposite- circular polarizations. (b) Simulated and theoretically calculated polarization conversion ratio.

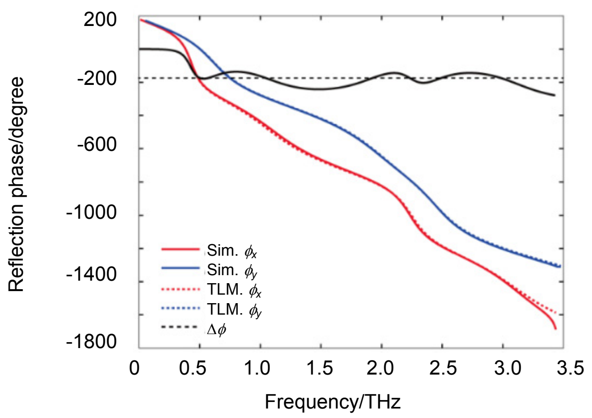

Fig.4 Simulated (solid line) and calculated (dash line) anisotropic dispersions of the metasurface and the phase difference $\Delta\phi$. TLM: transmission line model.

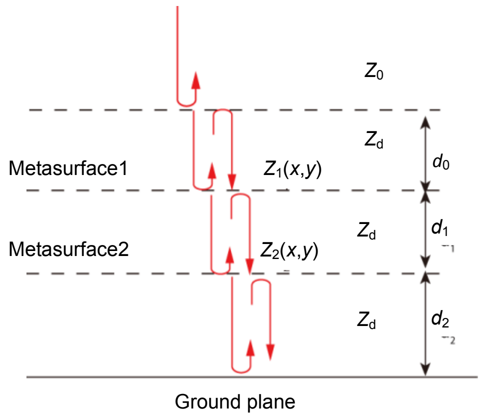

Fig.5 Schematic of the transmission line mode for achromatic polarization conversion.

DOI: 10.3969/j.issn.1003-501X.2017.01.008

$(L_{2,x}, C_{2,x}) = (1.4 \times 10^{-11}$ H, 1.8×10^{-15} F) and $(L_{2,y}, C_{2,y}) = (3 \times 10^{-11}$ H, 5.3×10^{-17} F). With these parameters, the calculated PCR is illustrated in Fig. 3, which agrees with the simulation results well. The impedances of the meta-atoms array are elucidated in Fig. 6, which can be taken as impedance-tuned interfaces with dramatically modified complex reflection and transmission coefficients. The achromatic performance is attributed to the conjugation compensation of the dispersion of metasurface and the thickness-dependent dispersion of the dielectric spacing layer.

The magnetic field distributions at the cross section of *x*-*z* plane are investigated and shown in Fig. 7. Obviously, the Metasurface 1 mainly responses to the *y*-component of higher frequencies while Metasurface 2 mainly responses to the *x*-component of lower frequencies. Moreover, each metasurface can interact with the incidence in a broad range. Therefore, the dispersion of the meta-mirror can be engineered in a broad range.

5 Conclusions

In summary, an anisotropic meta-mirror with cascading meta-atoms array has been proposed to behave as a half-wave plate. In order to obtain a broadband operation bandwidth beyond 2-octave band, the design principle of the cascading meta-atoms array follow the log-periodic configuration. In principle, the bandwidth can be further expanded by cascading more meta-atoms array or adopting more elaborate design for dispersion engineering. The proposed strategy may pave the way for the design of broadband metamaterial-based devices and in-

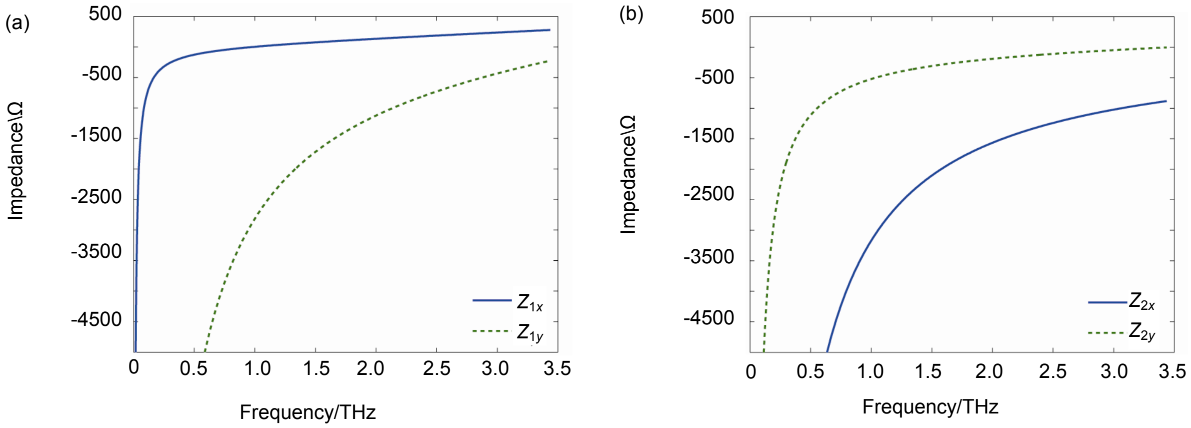

Fig.6 Retrieved impedance of (a) Metasurface 1 and (b) Metasurface 2 by equivalent circuit theory.

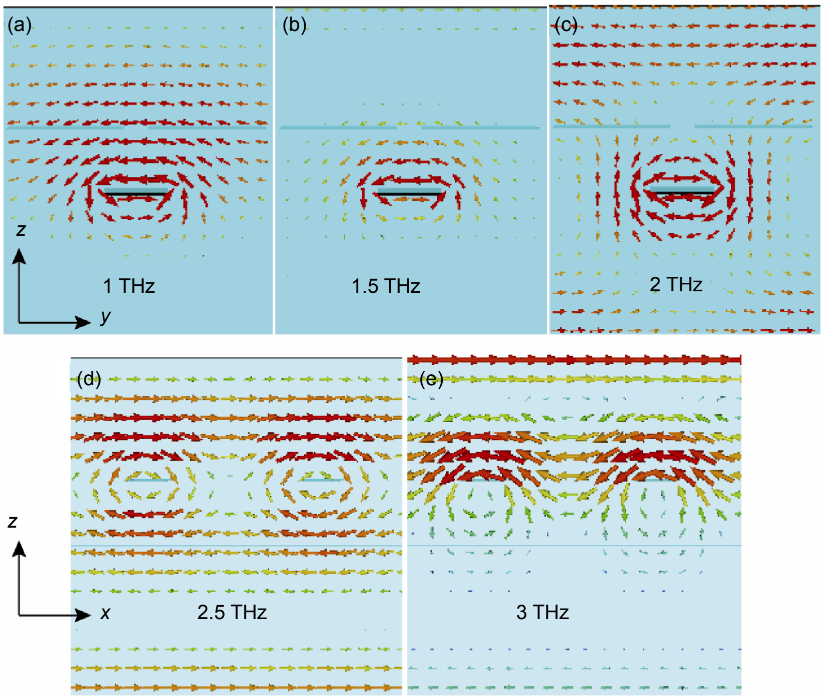

Fig.7 (a)~(e) Magnetic field distributions of the unit cell at frequencies of 1, 1.5, 2, 2.5 and 3 THz, respectively.

spire the applications in integrated photonics. Furthermore, by utilizing dynamic control method[2, 29], the performance of our device can be significantly improved.

Acknowledgements

The work was supported in part by National Science Foundation (NSF).

References

1 Flanders D C. Submicrometer periodicity gratings as artificial anisotropic dielectrics[J]. *Applied Physics Letters*, 1983, **42**(6): 492–494.

2 Ma Xiaoliang, Pan Wenbo, Huang Cheng, *et al*. An active metamaterial for polarization manipulating[J]. *Advanced Optical Materials*, 2014, **2**(10): 945–949.

3 Gansel J K, Thiel M, Rill M S, *et al*. Gold helix photonic metamaterial as broadband circular polarizer[J]. *Science*, 2009, **325**(5947): 1513–1515.

4 Yu Nanfang, Aieta F, Genevet P, *et al*. A broadband, background-free quarter-wave plate based on plasmonic metasurfaces[J]. *Nano Letters*, 2012, **12**(12): 6328–6333.

5 Luo Xiangang. Principles of electromagnetic waves in metasurfaces[J]. *Science China Physics, Mechanics & Astronomy*, 2015, **58**(9): 594201.

6 Luo Xiangang, Pu Mingbo, Ma Xiaoliang, *et al*. Taming the electromagnetic boundaries via metasurfaces: from theory and fabrication to functional devices[J]. *International Journal of Antennas and Propagation*, 2015, **2015**: 204127.

7 Sun Shulin, Yang Kuangyu, Wang C M, *et al*. High-efficiency broadband anomalous reflection by gradient meta-surfaces[J]. *Nano Letters*, 2012, **12**(12): 6223–6229.

8 Lin Jiao, Mueller J P B, Wang Qian, *et al*. Polarization-controlled tunable directional coupling of surface plasmon polaritons[J]. *Science*, 2013, **340**(6130): 331–334.

9 Lin Jiao, Wang Qian, Yuan Guanghui, *et al*. Mode-matching metasurfaces: coherent reconstruction and multiplexing of surface waves[J]. *Scientific Reports*, 2015, **5**: 10529.

10 Pu Mingbo, Li Xiong, Ma Xiaoliang, *et al*. Catenary optics for achromatic generation of perfect optical angular momentum[J]. *Science Advances*, 2015, **1**(9): e1500396.

11 Li Xiong, Pu Mingbo, Zhao Zeyu, *et al*. Catenary nanostructures as compact Bessel beam generators[J]. *Scientific Reports*, 2016, **6**: 20524.

12 Li Zhongyang, Palacios E, Butun S, *et al*. Visible-frequency metasurfaces for broadband anomalous reflection and high-efficiency spectrum splitting[J]. *Nano Letters*, 2015, **15**(3): 1615–1621.

13 Guo Yinghui, Pu Mingbo, Zhao Zeyu, *et al*. Merging geometric phase and plasmon retardation phase in continuously shaped metasurfaces for arbitrary orbital angular momentum generation[J]. *ACS Photonics*, 2016, 3(11): 2022–2029.

14 Guo Yinghui, Yan Lianshan, Pan Wei, *et al*. Generation and manipulation of orbital angular momentum by all-dielectric metasurfaces[J]. *Plasmonics*, 2016, **11**(1): 337–344.

15 Guo Yinghui, Yan Lianshan, Pan Wei, *et al*. Scattering engineering in continuously shaped metasurface: an approach for electromagnetic illusion[J]. *Scientific Reports*, 2016, **6**: 30154.

16 Sun Jingbo, Liu Lingyun, Dong Guoyan, *et al*. An extremely broad band metamaterial absorber based on destructive interference[J]. *Optics Express*, 2011, **19**(22): 21155–21162.

17 Cui Yanxia, Fung K H, Xu Jun, *et al*. Ultrabroadband light absorption by a sawtooth anisotropic metamaterial slab[J]. *Nano Letters*, 2012, **12**(3): 1443–1447.

18 Guo Yinghui, Yan Lianshan, Pan Wei, *et al*. Ultra-broadband terahertz absorbers based on 4 × 4 cascaded metal-dielectric pairs[J]. *Plasmonics*, 2014, **9**(4): 951–957.

19 Chin J Y, Gollub J N, Mock J J, *et al*. An efficient broadband metamaterial wave retarder[J]. *Optics Express*, 2009, **17**(9): 7640–7647.

20 Jen Y J, Lakhtakia A, Yu C W, *et al*. Biologically inspired achromatic waveplates for visible light[J]. *Nature Communications*, 2011, **2**: 363.

21 Rozanov K N. Ultimate thickness to bandwidth ratio of radar absorbers[J]. *IEEE Transactions on Antennas and Propagation*, 2000, **48**(8): 1230–1234.

22 Lier E, Werner D H, Scarborough C P, *et al*. An octave-bandwidth negligible-loss radiofrequency metamaterial[J]. *Nature Materials*, 2011, **10**(3): 216–222.

23 Feng Qin, Pu Mingbo, Hu Chenggang, *et al*. Engineering the dispersion of metamaterial surface for broadband infrared absorption[J]. *Optics Letters*, 2012, **37**(11): 2133–2135.

24 Li Yang, Li Xiong, Pu Mingbo, *et al*. Achromatic flat optical components via compensation between structure and material dispersions[J]. *Scientific Reports*, 2016, **6**: 19885.

25 Pu Mingbo, Chen Po, Wang Yanqin, *et al*. Anisotropic meta-mirror for achromatic electromagnetic polarization manipulation[J]. *Applied Physics Letters*, 2013, **102**(13): 131906.

26 Guo Yinghui, Wang Yanqin, Pu Mingbo, *et al*. Dispersion management of anisotropic metamirror for super-octave bandwidth polarization conversion[J]. *Scientific Reports*, 2015, **5**: 8434.

27 Guo Yinghui, Yan Lianshan, Pan Wei, *et al*. Achromatic polarization manipulation by dispersion management of anisotropic meta-mirror with dual-metasurface[J]. *Optics Express*, 2015, **23**(21): 27566–27575.

28 Wang Dacheng, Zhang Lingchao, Gu Yinghong, *et al*. Switchable ultrathin quarter-wave plate in terahertz using active phase-change metasurface[J]. *Scientific Reports*, 2015, **5**: 15020.

29 Wang Dacheng, Zhang Lingchao, Gong Yandong, *et al*. Multiband switchable terahertz quarter-wave plates via phase-change metasurfaces[J]. *IEEE Photonics Journal*, 2016, **8**(1): 5500308.

30 Jiang Shangchi, Xiong Xiang, Hu Yuansheng, *et al*. Controlling the polarization state of light with a dispersion-free metastructure[J]. *Physical Review X*, 2014, **4**(2): 021026.

31 Grady N K, Heyes J E, Chowdhury D R, *et al*. Terahertz metamaterials for linear polarization conversion and anomalous refraction[J]. *Science*, 2013, **340**(6138): 1304–1307.

32 Zhang Zuojun, Luo Jun, Song Maowen, *et al*. Large-area, broadband and high-efficiency near-infrared linear polarization manipulating metasurface fabricated by orthogonal interference lithography[J]. *Applied Physics Letters*, 2015, **107**(24): 241904.

33 Isbell D. Log periodic dipole arrays[J]. *IRE Transactions on Antennas and Propagation*, 1960, **8**(3): 260–267.

34 Carrel R. The design of log-periodic dipole antennas[C]. Proceedings of IRE International Convention Record, New York, NY, USA, 1961: 61–75.

35 Shelton P J. Wideband polarization-transforming electromagnetic mirror: US, 4228437[P]. 1980-10-14.